J|A|C|S ARTICLES

Published on Web 10/26/2009

Shape Control of CdSe Nanocrystals with Zinc Blende Structure

Liping Liu, Zhongbin Zhuang, Ting Xie, Yang-Gang Wang, Jun Li, Qing Peng, and Yadong Li*

State Key Laboratory of New Ceramics and Fine Processing; Department of Chemistry, Tsinghua University, Beijing, 100084 P.R. China

Received May 13, 2009; E-mail: ydli@mail.tsinghua.edu.cn

Abstract: Systematically shape-controlled synthesis of inorganic nanocrystals has attracted increasing attention recently for both fundamental and technological interest. The shape evolution of CdSe nanocrystals with wurtzite structure in a unified method has been previously well studied, while the study on shape evolution of CdSe nanocrystals with zinc blende structure still remains challenging. Here, we demonstrate a systematic shape variation of zinc blende CdSe nanocrystals in a modified organometallic approach, in which distinct shapes of cube-shaped, sphere-shaped, tetrahedron-shaped, and branched CdSe nanocrystals with high yield and good uniformity are obtained. The crucial factor that influences the shape-controlled process is the reactive temperature. This wide variation of shapes provides important information about the growth of CdSe nanocrystals, and it can also help in the shape-controlled synthesis of other nanocrystals that are bound with uniform crystal planes.

Introduction

The study of shape-controlled synthesis of colloid nanocrystals has become active since it was first reported that the wurtzite phase CdSe nanocrystals with elongated rod shape and other anisotropic growth shapes, such as arrows, teardrops, and tetrapods, could be prepared by tuning the reactive parameters.[1,2] In later reports, some approaches have focused on the mechanism of anisotropic growth and precious shape-controlled study.[3−8] Strong binding ligands were first found that could lead to the formation of CdSe nanorods,[1] and then the monomer concentration of the precursors in solution was found to be a determining factor in the shape-controlled process according to Peng.[3,6] Meanwhile, Sapra et al. found that the reactive temperature and the nature of the ligands also played important roles in the transformation between sphere-shaped and rod-shaped CdSe nanocrystals.[8] With these previous studies, the formation mechanism of one-dimensional CdSe nanocrystals is gradually established, and the knowledge gained from these studies has been applied to guide the shape-controlled synthesis of other semiconductor nanocrystals.[9−12] In these studies, the crystalline structures of CdSe nanocrystals with various elongated shapes all belong to the hexagonal wurtzite phase, while the study of CdSe nanocrystals with cubic zinc blende structure is seldom reported. Herein, we demonstrate the shape evolution of zinc blende CdSe nanocrystals in a modified organometallic approach, by reacting element Se with $Cd(Ac)_2$ in the presence of oleic acid.

In our synthetic approach, elemental Se powder is chosen as the Se source. Se powder can disperse in octadecene (ODE) when the temperature is higher than its melting point (~217 °C) and becomes chemically active. In the absence of a selenium passivant and using fatty acid as the sole capping ligand, it can often lead to the formation of CdSe nanocrystals with zinc blende structure.[13,14] For the wurtzite CdSe nanocrystals, their intrinsic cell structure possesses a unique *c*-axis. This kind of anisotropic unit cell can induce anisotropic growth along the crystalline reactive direction (*c*-axis), and therefore, elongated shapes of CdSe nanocrystals are expected by controlling the key reactive parameters such as monomer concentrations or the nature of the capping ligands as mentioned above.[2,6,8] For the CdSe with zinc blende structure, its crystal has an isotropic unit cell structure, which may probably lead to the formation of nanocrystals with isotropic structures like cube, tetrahedron, and so on. Also, due to the intrinsic distinguishing thermodynamic difference on different planes of the crystal with zinc blende structure, we found that the most influential factor in shape control here was the reactive temperature. In the thermodynamic dominated crystal growth region, the atoms would likely grow

(1) Peng, X. G.; Manna, L.; Yang, W. D.; Wickham, J.; Scher, E.; Kadavanich, A.; Alivisatos, A. P. *Nature* **2000**, *404*, 59.
(2) Manna, L.; Scher, E. C.; Alivisatos, A. P. *J. Am. Chem. Soc.* **2000**, *122*, 12700.
(3) Peng, Z. A.; Peng, X. G. *J. Am. Chem. Soc.* **2001**, *123*, 1389.
(4) Peng, Z. A.; Peng, X. G. *J. Am. Chem. Soc.* **2002**, *124*, 3343.
(5) Lee, S. M.; Cho, S. N.; Cheon, J. *Adv. Mater.* **2003**, *15*, 441.
(6) Peng, X. G. *Adv. Mater.* **2003**, *15*, 459.
(7) Manna, L.; Milliron, D. J.; Meisel, A.; Scher, E. C.; Alivisatos, A. P. *Nat. Mater.* **2003**, *2*, 382.
(8) Sapra, S.; Poppe, J.; Eychmuller, A. *Small* **2007**, *3*, 1886.
(9) Yu, W. W.; Peng, X. G. *Angew. Chem., Int. Ed.* **2002**, *41*, 2368.
(10) Jun, Y. W.; Lee, S. M.; Kang, N. J.; Cheon, J. *J. Am. Chem. Soc.* **2001**, *123*, 5150.
(11) Wang, L. Y.; Li, P.; Zhuang, J.; Bai, F.; Feng, J.; Yan, X. Y.; Li, Y. D. *Angew. Chem., Int. Ed.* **2008**, *47*, 1054.
(12) Viswanatha, R.; Battaglia, D. M.; Curtis, M. E.; Mishima, T. D.; Johnson, M. B.; Peng, X. G. *Nano Res.* **2008**, *1*, 138.
(13) Jasieniak, J.; Bullen, C.; Embden, J. V.; Mulvaney, P. *J. Phys. Chem. B* **2005**, *109*, 20665.
(14) Yang, Y. A.; Wu, H. M.; Williams, K. R.; Cao, Y. C. *Angew. Chem., Int. Ed.* **2005**, *44*, 6712.

on a crystal facet that has higher surface energy to lower the overall energy of the crystal. At the same time, in a nanocrystal growth process, the capping ligands dynamically adsorb and desorb from the nanocrystal surface,[15−17] enabling the addition or the removal of the atoms from the crystallites. Since reactive temperature directly influences the dynamics of the capping ligands, it can naturally influence the growth of atoms on different crystal facets in different surface absorption situations, and then control the final shape of the products. Thus, by controlling the reactive temperature, distinct cube-shaped, sphere-shaped, tetrahedron-shaped, and branched CdSe nanocrystals with high yield and good uniformity are obtained.

Experimental Section

Materials. The reagents used in this work, including Se powder, $Cd(Ac)_2 \cdot 2H_2O$, oleic acid, n-hexane, and ethanol, were A. R. grade (>99.99%) from the Beijing Chemical Factory, China. The octadecene (ODE) (90%, Tech.) was purchased from J&K Chemical Ltd. The chemicals were used directly without any purification.

Synthesis. For the synthesis of sphere CdSe nanocrystals, 0.0784 g (1 mmol) of Se powder and 15 mL of ODE were loaded into a 50 mL flask, and then it was heated to 280 °C for half an hour to get an apparent clear yellow solution. A 0.266 g portion of $Cd(Ac)_2 \cdot 2H_2O$ and 5 mL of oleic acid were mixed together in a beaker and heated to 120 °C to get a transparent solution, and then it was swiftly added to the Se stock solution. The temperature dropped to 248−249 °C after the Cd-precursor solution was added, and then it quickly raised to about 260 °C by adjusting the power of the heating mantle. The temperature adjusted process can be finished in 1 min. During the whole reaction process, the temperature was maintained at 260 ± 1 °C for the growth of the nanocrystals. Aliquots were taken at different time intervals, and UV−vis and PL spectra were recorded for each aliquot. After about 40 min of reaction time, the flask was taken out of the heating mantle. Ethanol was added to the reactive solution to precipitate the nanocrystals, and then the nanocrystals were collected by centrifugation. Finally, the CdSe nanocrystals were redissolved in n-hexane. The synthesis process of CdSe nanocrystals with cube, tetrahedron, and branched shapes was similar to that of sphere CdSe nanocrystals except for the reactive temperature. For instance, to synthesize cube-shaped CdSe nanocrystals, the Cd-precursor solution was first held at 150 °C, and then after it was added to the flask, the temperature of the reactive solution dropped to around 262 °C; it can be adjusted to 275 °C for the growth of the nanocrystals in 1 min. For the synthesis of tetrahedron and branched CdSe nanocrystals, the crystal was allowed to grow at 250 and 240 °C, respectively.

Theoretical Details. The theoretical calculations of the surface energies and the adsorption energies were performed by using the DMol^3 program (version 4.0) developed by Accelrys Inc.[18−20] We chose to use the generalized-gradient approximation (GGA) with the PBE functional.[21] The double numerical plus polarization (DNP) basis set was used to describe the valence orbitals of the atoms, whereas relativistic effective core potentials (ECP) were employed for replacing the [$1s^2-3d^{10}$] core electrons of Cd and Se atoms.[18,20] In all the calculations, stoichiometric supercell models were used, with an 8 × 8 × 8 k-point mesh for the bulk crystal and an 8 × 8 × 1 k-point mesh for the slabs. All the slabs were repeated periodically with a vacuum spacing of 15 Å` between the images. In the geometry optimizations the total energy was converged to 0.001 eV. The calculated lattice constant is 6.23 Å, close to the experiment constant 6.08 Å, indicating that the selected exchange-correlation functional is appropriate.

The surface energies were determined using the slab method in which surface energies were obtained by

$$E_{surf} = 1/2[E_{slab} - nE_b]/A$$

where A is the area of the supercell, E_b is the bulk energy per unit cell with a formula Cd_4Se_4, and E_{slab} is the energy per surface unit cell of the specified slab model, which contains n bulk unit cells. The factor $^1/_2$ represents that the two surfaces of the slab were taken into consideration. In these calculations, the (001), (111), and (11$\bar{1}$) surfaces were both modeled with 2 × 2 supercell slabs consisting of 16 atomic layers. The two top layers and two bottom layers were allowed to relax, and all other layers were kept fixed. Each of these slab models contains 32 Cd atoms and 32 Se atoms.

The adsorption energy was calculated as follows:

$$E_{adsorption} = -(E_{slab+adsorbate} - E_{slab} - E_{adsorbate})$$

where $E_{slab+adsorbate}$ is the energy of the adsorption complex including the relaxed surface and the adsorbate molecule, and $E_{adsorbate}$ is the energy of the isolated adsorbate molecule. The clean (001) and (111) surfaces consist of eight atomic layers. Each of these surfaces contains 16 Cd atoms and 16 Se atoms. The two top layers of the substrate were allowed to relax, and all other bottom layers were kept fixed. Since the adsorbent bonding for a carboxylic acid may involve either one oxygen atom (the monodentate structure) or two oxygen atoms (the bidentate structures), both the monodentate and bidentate structures were considered and calculated. Acetic acid was used as a simple model molecule to investigate the binding behavior of oleic acid adsorbed on the CdSe surfaces, as this binding can mainly be attributed to the interaction between the carboxyl functional group and the surface. Acetic acid has been considered as a representative carboxylic acid that was shown to adsorb on metal and metal oxide surfaces.[22,23]

Characterization. The CdSe nanocrystals were determined by using transmission electron microscopy (TEM, JEOL JEM 1200EX working at 100 kV), high resolution transmission electron microscopy (HRTEM, FEI Tecnai G2 F20 S-Twin working at 200 kV), and scanning electron transmission microscopy (STEM, FEI Tecnai G2 F20 S-Twin working at 200 kV). The electronic absorption spectra were obtained on a Hitachi U-3010 UV−vis spectrometer, and the luminescence spectra were recorded with a Hitachi F-4500 fluorescence spectrophotometer. The phases of the products were examined by XRD on a Bruker D8 Advance X-ray powder diffractometer with the Cu Kα radiation (λ = 1.5418 Å). The theoretical details are shown in the Supporting Information.

Results and Discussion

The TEM images in Figure 1a,b show the CdSe products with sphere shape when the crystal growth temperature was set as 260 °C (see more details in the Experimental Section). Without size sorting, the spherical CdSe nanocrystals obtained here showed good monodispersity with an average diameter of 4.5 nm and a standard deviation (σ) of 7%. They could easily assemble together to form a 2D structure when dropped on the carbon-supported copper grid with an appropriate concentration as shown in Figure 1a. The XRD image of the spherical CdSe nanocrystals is displayed in Figure 2 (A pattern). Although the two crystal phases (wurtzite and zinc blende structure) of CdSe

(15) Murray, C. B.; Kagan, C. R.; Bawendi, M. G. *Annu. Rev. Mater. Sci.* **2000**, *30*, 545.
(16) Pradhan, N.; Reifsnyder, D.; Xie, R. G.; Aldana, J.; Peng, X. G. *J. Am. Chem. Soc.* **2007**, *129*, 9500.
(17) Liu, L. P.; Peng, Q.; Li, Y. D. *Inorg. Chem.* **2008**, *47*, 5022.
(18) Delley, B. *J. Chem. Phys.* **1990**, *92*, 508.
(19) Delley, B. *J. Phys. Chem.* **1996**, *100*, 6107.
(20) Delley, B. *J. Chem. Phys.* **2000**, *113*, 7756.
(21) Perdew, J. P.; Burke, K.; Ernzerhof, M. *Phys. Rev. Lett.* **1996**, *77*, 3865.
(22) McGill, P. R.; Idriss, H. *Surf. Sci.* **2008**, *602*, 3688.
(23) Hwang, E.; Kim, D. H.; Hwang, Y. J.; Kim, A.; Hong, S.; Kim, S. *J. Phys. Chem. C* **2007**, *111*, 5941.

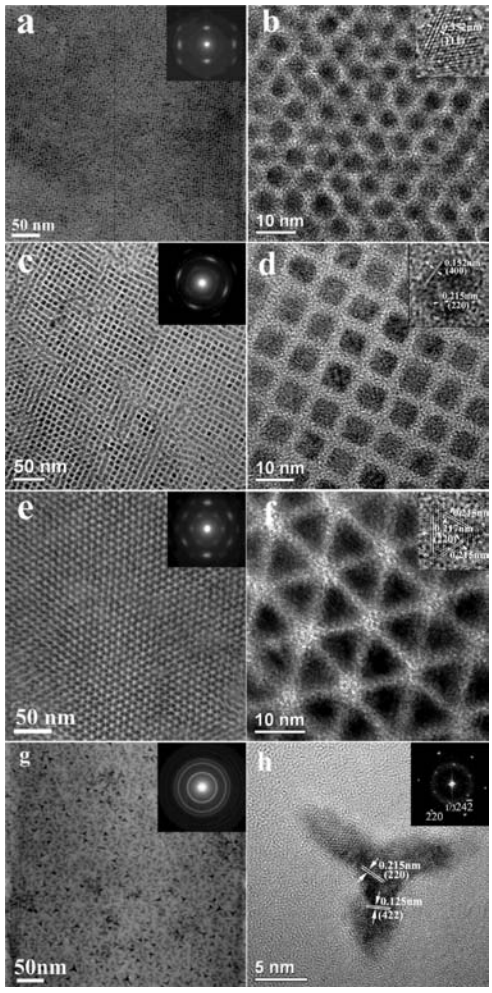

Figure 1. TEM images of the CdSe nanocrystals with different shapes: (a, b) sphere-shaped; (c, d) cube-shaped; (e, f) tetrahedron-shaped; (g, h) branched. The inset images in parts a, c, d, and g are the SAED patterns of the corresponding samples.

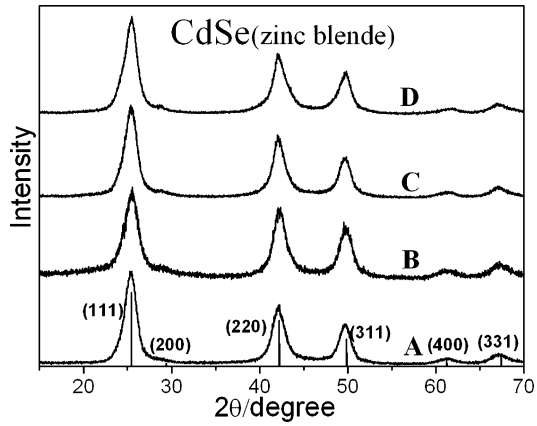

Figure 2. XRD patterns of CdSe nanocrystals with (A) sphere, (B) cube, (C) tetrahedron, and (D) branched shapes.

have similar XRD results as the nanocrystals,[13] the XRD pattern here unambiguously indicates that these CdSe products have a zinc blende structure: (a) the pattern at around 35° and 45° 2θ angle is flat and deep, where (102) and (103) reflection peaks would have existed if the CdSe had the wurtzite structure; (b) there is a characteristic (400) reflection peak appeared at around 61° for the CdSe with zinc blende structure. The other main diffraction peaks can also match well with the zinc blende CdSe reflections (JCPDS 65−2891).

Sphere-shaped CdSe nanocrystals can be considered as the first morphology in a thermodynamically dominated growth regime since the sphere shape has a low overall surface area and thus has the low surface energy. The formation of an isotropic sphere shape also indicates that the different adsorption energies of the capping ligands on different crystal planes are not important in crystal growth process at this temperature; thus, it provides the opportunity for the reconstruction of the surface atoms to lower the surface energy if thermal energy is supported. As in a spherical single-crystalline crystal, its surface must contain high-index crystallography planes, which possibly result in a higher surface energy, thus giving more energy, or without the strongly adhering of the capping ligands, facets tend to form on the crystal surface to increase the portion of the low-index planes.[24] When we extended the reactive time to 3 h at 260 °C in the experiment, these spherical CdSe nanocrystals began to change to truncated octahedrons although the size distribution was broadened (Figure 3a). Therefore, by increasing the reactive temperature, the rate of ligands attaching and detaching to the surface of the nanocrystals is faster, which will give more chances for the atoms to grow on the crystal surface to produce low-index crystallography planes, and polyhedrons with thermodynamical stable planes will form.

Figure 1c,d shows the CdSe products when the reactive temperature is increased to 275 °C. It can be seen that the products are composed of nearly monodispersed cubic nanocrystals with a diameter of 6 nm, and they can also easily self-assemble to 2D arrays on the TEM grid due to their uniform shape. As discussed above, when sufficient thermal energy is supplied at high growth temperature (275 °C), the attaching and detaching rates of the ligands are fast due to the weak binding between the ligands and the nanocrystals. The surface energy consideration is crucial in understanding and predicting the morphology of the nanocrystals; stable morphology where surface energy is minimized will prevail during the formation of the nanocrystals.[25] For the zinc blende phase CdSe crystal, we calculated the intrinsic surface energies of different planes using relativistic density functional theory (DFT), and the results are listed in Table 1. The surface energies calculated from this slab geometry model are the average surface energy of the corresponding {001} and {111} facets; a more accurate calculation for each individual surface energy can be obtained from the wedge-shaped geometry model which was developed by Zhang and Wei.[26−28] Here, we used these average surface energies to evaluate the dominated thermodynamic growth direction between the {001} and {111} facets.[29] The details of the calculation methods are described in the Experimental Section. The theoretical results show that the surface energy of the {111} planes is larger than that of the {100} planes because of the higher packing density and the number of unsaturated atoms on the {111} facets in its intrinsic structure (Figure 3b−e). Thus, at the reactive temperature of 275 °C, the growth of atoms on the {111} facets was favored. The stacking of atoms on the

(24) Wang, Z. L. *J. Phys. Chem. B* **2000**, *104*, 1153.
(25) Tao, A. R.; Habas, S.; Yang, P. D. *Small* **2008**, *4*, 310.
(26) Zhang, S. B.; Wei, S. H. *Phys. Rev. Lett.* **2004**, *92*, 086102.
(27) Rempel, J. Y.; Trout, B. L.; Bawendi, M. G.; Jensen, K. F. *J. Phys. Chem. B* **2005**, *109*, 6183.
(28) Manna, L.; Wang, W. L.; Cingolani, R.; Alivisatos, A. P. *J. Phys. Chem. B* **2005**, *109*, 19320.
(29) Lee, S. M.; Jun, Y. W.; Cho, S. N.; Cheon, J. *J. Am. Chem. Soc.* **2002**, *124*, 11244.

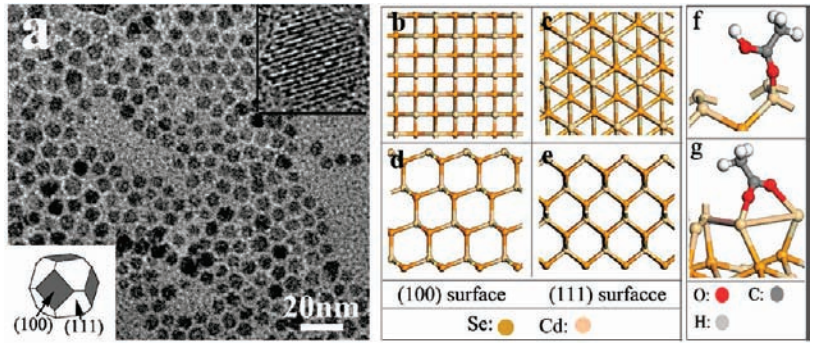

Figure 3. (a) TEM image of spherically shaped truncated octahedrons. (b−e) Schematic diagrams of surface atom arrangement on CdSe surface: (b) top view and (d) side view of (100) surface; (c) top view and (e) side view of (111) surface. (f, g) Sketch maps of adsorbent (f) monodentate structure and the (g) bidentate structure (acetic acid was used to represent the oleic acid as they had the same carboxyl functional group[22,23]).

Table 1. Calculated Average Surface Energies and Absorption Energies on {100} and {111} Surfaces of the Zinc Blende CdSe Crystal[a]

surface index	(100)	(111)
surface energy (J/m^2)	0.83	0.91
$E_{adsorption}$ (eV)	0.37 (M), 0.45 (B)	1.01(M), 1.36 (B)

[a] For the absorption energies, the letter M means monodentate structure and the letter B means bidentate structures.

{111} facets led to the disappearance of these planes, and then CdSe nanocrystals with cubic shape were obtained from the truncated octahedrons. The fringe spacing parallel to the edge and the diagonal of the square observed in the inset of Figure 2c could also be indexed as the separation for the {400} and {220} planes as other normal cubic nanocrystals with face-centered cubic (fcc) structure.

When the reactive temperature depresses, the capping ligands stay on the nanocrystals more steadily, and the effect of different adsorption energies of capping ligands on different crystal planes emerges in the crystals growth process. The calculated results in Table 1 show that the adsorption energy (see more details in the Theoretical Details subsection of the Experimental Section) of the {100} facets is lower than that of the {111} facets, indicating that the growth of the atoms on the {100} facets should have a lower activation energy barrier. During the growth of a crystal, preferential growth is facilitated along the kinetically most favorable direction with low activation energy barriers. Tetrahedron-shaped CdSe nanocrystals were obtained when the crystal growth temperature was depressed to 250 °C. The morphology of the products was shown in Figure 1e,f, and the size of the CdSe nanocrystals was about 8 nm. The inset SAED pattern displayed in Figure 1e confirms the well self-assembled state of the CdSe nanocrystals, and the hexagonal symmetry of these spot patterns implies that the underside facets of these nanocrystals are all bounded by the {111} planes. Although these products seemed to have a triangular shape in the TEM image, analytical STEM studies revealed that these nanocrystals actually had a tetrahedral structure rather than a trianglar structure (Figure 4a), and the line elemental EDS data across one single nanocrystal also confirmed this tetrahedral structure (Figure 4b,c).[30] These tetrahedron CdSe nanocrystals may mainly evolve from the seeds with a fixed (111) base and exposed three {111} and {100} facets.[24] The growth on the {100} facets was faster since it was easier than on the {111} planes at this relatively low temperature. With the stacking of the atoms on the {100} facets, the area ratio of {111} to {100} gradually increased, and finally resulted in the formation of the tetrahedron shape. The formation of tetrahedrons instead of octahedrons may be due to the shape of their seeds being different with the temperature. The inset of Figure 1f shows the HRTEM image of an individual CdSe tetrahedron. The fringe spacing of 0.215 nm parallel to the three edges of the triangle can be indexed to the {220} interplane distance for zinc blende CdSe.

When the reactive temperature was continued to depress to 240 °C, we got the branch-shaped CdSe nanocrystals. It can be seen that these nanocrystals all possess three branches out of the crystal center (Figure 1g,h). A more detailed measurement was operated by rotating the sample in TEM to observe their exact morphologies: we found that there were only three branches or less out of each crystal, without formation of a tetrapod structure. In addition, different from the multipod-shaped CdSe nanocrystals, which were generated through controlled nucleation of a zinc blende phase core followed by the growth of wurtzite phase arms, the powder XRD pattern (Figure 2, D pattern) proved that these anisotropic structure products had a zinc blende structure. The inset of Figure 1h was the fast Fourier transform (FFT) of the corresponding individual sample in Figure 1h. The hexagonal symmetry of these spot patterns indicated that the sample was projected along the [111] direction and with a bottom covered with the (111) facets. There are two sets of spots that could be identified on the basis of their *d*-spacing: the outer set with a spacing of 0.215 nm could be indexed to the {220} interplane distance. The inner set with a lattice spacing of 0.373 nm was believed to originate from the ($^1/_3$){422} Bragg reflections, which is normally forbidden by an fcc lattice. These forbidden ($^1/_3$){422} reflections have been previously observed in Au or Ag nanocrystals with fcc structures.[31] The appearance of the forbidden ($^1/_3$){422} reflection in the fcc structure nanocrystal is mainly caused by the intrinsic defects in the nanocrystal, and there are two kinds of familiar modalities that lead to the formation of the ($^1/_3$){422} reflection:[31] (a) nanocrystals with slice shapes, as they always contain a number of nonintegral fcc cells on the surface; and (b) nanocrystals with more than two twins on the {111} plane, because the twins will break the integrated structure of the crystals. Since the intensity of the ($^1/_3$){422} reflection caused by the slice nanocrystals is weak (usually lower than 10^{-2} of the principal reflections), the ($^1/_3$){422} reflection here was

(30) Koo, B.; Patel, R. N.; Korgel, B. A. *J. Am. Chem. Soc.* **2009**, *131*, 3134.

(31) Kirkland, A. I.; Jefferson, D. A.; Duff, D. G.; Edwards, P. P.; Gameson, I.; Johnson, B. F. G.; Smith, D. *Proc. R. Soc. London, Ser. A* **1993**, *440*, 589.

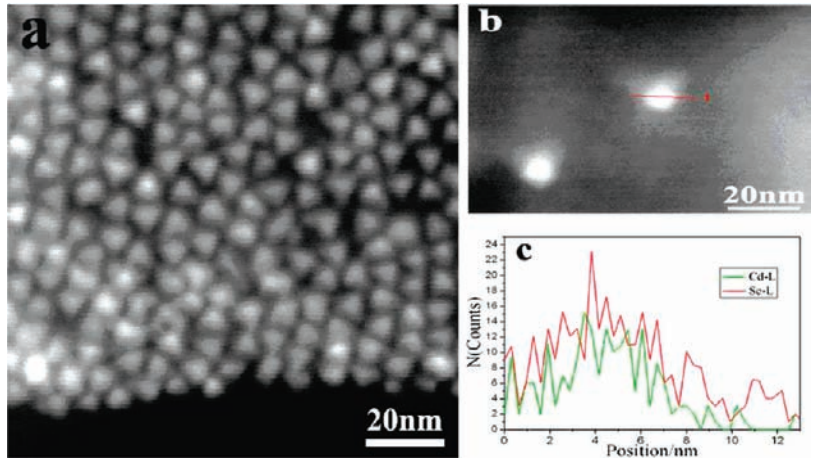

Figure 4. (a) High angle annular dark field image of tetrahedral CdSe nanocrystals. (c) Corresponding elemental profiles for Se and Cd obtained by recording EDS signal intensities along the line shown in red in panel b.

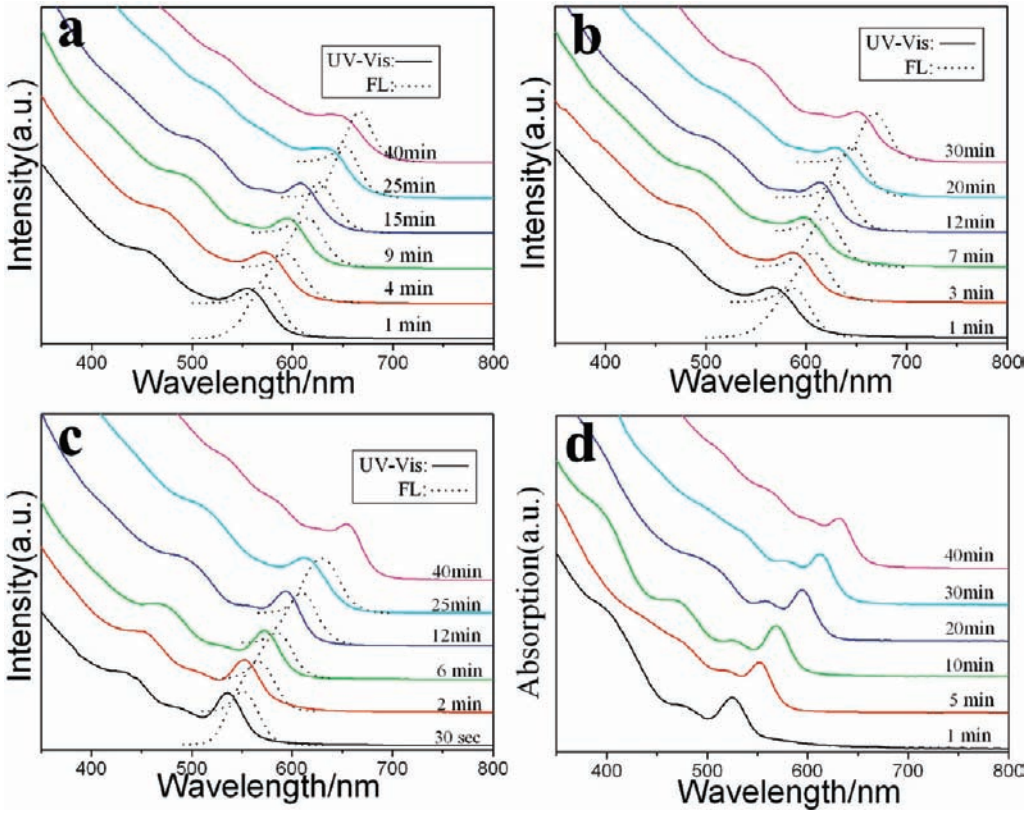

Figure 5. Temporal evolution of the UV−vis and photoluminescence (PL) spectrum of CdSe nanocrystals with various shapes: (a) sphere-shaped, (b) cube-shaped, (c) tetrahedron-shaped, and (d) branched.

supposed to be caused by the existence of twins in the nanocrystal, which can also influence the optical property of this kind of product. In the formation of this branched structure, the branches growing along the ⟨211⟩ directions may also be a kinetically favored direction because the atom packing density is low on the {211} facets and thus has low density of the capping ligands. It was easy for the Se atoms to react with Cd atoms as there was not much steric hindrance effect on these facets. When we depressed the concentration of the precursors to half of the amounts described in the Experimental Section, that is, to about 0.025 M for Se and Cd, we still could get the branch-shaped CdSe nanocrystals. Thus, the concentration of the precursors here did not act as the main reason for the formation of the complicated shape. Kinetically controlled growth may play the most important role in determining the shape of the nanocrystals.

On the basis of the discussion of the formation of these four differently shaped CdSe nanocrystals, we could find out that the temperature was mostly controlling the dynamics of the capping ligands to influence the final shape of the product. At the temperature of 275 °C, the thermodynamic energy was high enough to make the ligands adsorb and desorb from the crystal surface frequently and nondistinctively; at this time, crystals were easily exposed to the ambient environment without the protection of the ligands. Thus, the atoms would selectively stack on {111} facets since {111} facets were more active, forming

cubic CdSe nanocrystals with only {100} facets. When the temperature depressed, at 260 °C, the thermodynamic energy was still high enough to desorb the capping ligands nondistinctively, but not that frequently. The atoms could add to the crystal only when the ligands desorbed from the crystal, which would lead to a similar growth rate in each facet of the crystal. Thus, the spherical shape with low overall surface area was favored.[24] When we went on depressing the reactive temperature, the kinetic factor would dominate the crystal growth process. At the temperature of 250 °C, the absorption of the ligands on {111} facets seemed more stable than that of {100} facets since the absorption energy on {111} facets was higher. The atoms would easily grow on {100} facets as the ligands on these facets could more easily desorb from the crystals. With the growth of the atoms on the {100} facets, the {100} facets gradually vanished, leaving {111} facets; thus, we got the tetrahedron-shaped CdSe nanocrystals. When at even lower temperature, 240 °C, the thermodynamic energy was not high enough to activate the capping ligands; at this time, the ligands stayed stable on the surface of the crystals. Then, a kinetically controlled growth on a less steric hindrance effect direction was favored, and branch-shaped CdSe nanocrystals with arm growth on ⟨211⟩ direction were formed.

Besides the morphology, we found that the specific surface area of the products were also temperature-dependent although their sizes were not. The experiment results showed that specific surface area of CdSe nanocrystals is depressed when the temperature is increased. The specific surface areas of the CdSe nanocrystals with cube, sphere, tetrahedron, and branch shapes are 1, 1.33, 1.83, and 1.91 nm^{-1}, respectively. Herein, to qualitatively interpret this phenomenon we cite the surface chemical thermodynamics (SCT) model,[32,33] which is developed on the basis of the fundamental equation of surface chemical thermodynamics (eq 1):

$$dG = -S\,dT + V\,dp + \gamma\,d\sigma + \sum_{i=1}^{n}\mu_{Bi}\,dn_{Bi} \qquad (1)$$

where γ is the specific surface energy, σ is the surface area, and μ is chemical potential. Under high adsorbate coverage, γ is proved to be dominated by the chemical potential of the adsorbate (μ_{ads}), which means (eq 2)[34]

$$\gamma \approx \gamma_0 - (\mu_{ads} - \mu'_{ads})\Gamma_{max} \qquad (2)$$

where γ_0 refers to the specific surface energy of the pristine interfaces, μ'_{ads} equals the value of μ_{ads} when $\gamma = \gamma_0$, and Γ_{max} is the saturated surface adsorbate density. The excess of oleic acid in the solution resulted in a tremendous absolute value of μ_{ads}, which led to $\gamma < 0$ (see more details in the Supporting Information).[34,35] To further simplify this SCT model, we integrate eq 1 into the following formula under the condition that the pressure (p) and the raw materials (n_B) are unchanged:

$$\Delta G = -S\Delta T + \gamma\Delta\sigma + \int_i^f \sum_{i=1}^{n}\mu_{Bi}\,dn_{Bi} \qquad (3)$$

As the morphology of the CdSe nanocrystals can be maintained for a long time after the reaction processed for about 45 min, which could be considered as an approximate equilibrium state, we have $\Delta G = 0$. At this time, the materials in solution were kept unchanged, i.e., $dn_B = 0$, and eq 4 follows:

$$-\gamma\Delta\sigma = -S\Delta T \qquad (4)$$

where $\Delta T > 0$, $\gamma < 0$ as discussed above, Then we can easily reach the conclusion (eq 5):

$$\Delta\sigma = \frac{-S\Delta T}{-\gamma} < 0 \qquad (5)$$

The above inequality reveals that the specific surface area of the CdSe nanocrystal decreases with the increase of the reactive temperature, which agrees well with the experimental results. Also, it showed that the CdSe nanocrystals tended to change to a thermodynamically stable structure when the temperature increased in this reactive condition.

Figure 5 shows the temporal evolution of the UV−vis and photoluminescence (PL) spectra of these four kinds of CdSe nanocrystal products. It can be seen that the optical property of the sphere-shaped and cube-shaped products is similar. The PL property of the tetrahedral CdSe nanocrystals shows little difference as the PL efficiency is gradually depressed when the reaction time (after 30 min) is extended, from about 12% to 2%. The fluorescence quenching phenomenon may probably be caused by the existence of the surface defects since the atoms could not grow on the nanocrystal as freely as they did at a high reactive temperature. For the branch-shaped CdSe nanocrystals, their fluorescence always vanished after the crystals grew for a few minutes. The reason may be due to the existence of the twin defects in the crystal as these stacking defects can act as efficient nonradiative recombination centers which could easily quench the fluorescence.[36,37] The absorption property of the branched CdSe was similar to those of the sphere- or cube-shaped CdSe nanocrystals. While comparing the position of the first absorption peaks and the final sizes of the CdSe nanocrystals with various shapes, it is found that although the overall size of the branch-shaped CdSe was larger than that of sphere or cube CdSe nanocrystals, they have more or less the same position for the first absorption peak. According to Scholes' work,[38] for these multipod-shaped nanocrystals, the excitons would mostly be confined in the narrow and long arms that extended from the small center. Thus, we can figure out that the first absorption of the branch-shaped CdSe nanocrystals is mostly derived from the actual smaller confinement volume of the arms.

Conclusion

In summary, we successfully synthesized high quality zinc blende CdSe nanocrystals with sphere, cube, tetrahedron, and branched shapes in a unified method. The formation of various

(32) Xie, T.; Li, S.; Peng, Q.; Li, Y. D. *Angew. Chem., Int. Ed.* **2009**, *48*, 196.
(33) Xie, T.; Li, S.; Wang, W. B.; Peng, Q.; Li, Y. D. *Chem.—Eur. J.* **2008**, *14*, 9730.
(34) Lin, Z.; Gilbert, B.; Liu, Q. L.; Ren, G. Q.; Huang, F. *J. Am. Chem. Soc.* **2006**, *128*, 6126.
(35) Lodziana, Z.; Topsoe, N. Y.; Norskov, J. K. *Nat. Mater.* **2004**, *3*, 289.
(36) DePuydt, J. M.; Haase, M. A.; Guha, S.; Qiu, J.; Cheng, H.; Wu, B. J.; Hofler, G. E.; Meis-Haugen, G.; Hagedorn, M. S.; Baude, P. F. *J. Cryst. Growth* **1994**, *138*, 667.
(37) Blanton, S. A.; Hines, M. A.; Guyot-Sionnest, P. *Appl. Phys. Lett.* **1996**, *69*, 3905.
(38) Kim, J.; Nair, P. S.; Wong, C. Y.; Scholes, G. D. *Nano Lett.* **2007**, *7*, 3884.

shapes of the CdSe nanocrystals was studied in detail, and the reactive temperature here was found to be the most influential factor in shape control process since it could influence the dynamics of the capping ligands and the growth of atoms on different crystal facets. Besides the morphology, specific surface area of the products was also temperature-dependent; that is, the specific surface area decreased when the reactive temperature increased, indicating a thermodynamic stabilization trend. The wide variation of different shapes for zinc blende CdSe presented here provides important information about the growth of nanocrystals in different thermodynamic situations, and it can also help in the shape-controlled synthesis of other nanocrystals bounded with uniform crystal planes, which may have potential application in the catalytic field.

Acknowledgment. This work was supported by NSFC (90606006, 20525104), the State Key Project of Fundamental Research for Nanoscience and Nanotechnology (2006CB932300), and the Key grant Project of Chinese Ministry of Education (306020).

Supporting Information Available: Temperature-dependent specific surface area evolution mechanism of CdSe nanocrystals. This material is available free of charge via the Internet at http://pubs.acs.org.

JA903633D